8TH CANADIAN MASONRY SYMPOSIUM

Jasper, Alberta
May 31 - June 3, 1998

THE INFLUENCE OF LIME AND METHYL CELLULOSE ON THE MICROSTRUCTURE AND BOND STRENGTH OF MORTARS IN COMBINATION WITH CALCIUM SILICATE UNITS

H.O. Sugo
Postgraduate Student, Department of Civil, Surveying and Environmental Engineering,
The University of Newcastle, Callaghan, NSW 2308, Australia

A.W. Page
CBPI Professor in Structural Clay Brickwork, Dean, Faculty of Engineering,
The University of Newcastle, Callaghan, NSW 2308, Australia

S.J. Lawrence
Senior Principal Research Scientist, CSIRO Building, Construction & Engineering,
PO Box 310, North Ryde, NSW 2113, Australia

ABSTRACT

This study investigates the mortar bond strengths and microstructures developed using Portland cement based mortars and calcium silicate masonry units. Bond strengths were determined using small cores tested in uniaxial tension which also allowed the evaluation of the mortar microstructure using optical and scanning electron microscopy. X-ray Diffraction and Thermal Analysis techniques were also used to identify the mortar constituents. The 1:1:6 mortar developed the greatest bond strength. The SEM/XRD work also indicated the Portland cement constituents to be more reacted for this mortar. Lime and methyl cellulose improved the retention of moisture by the mortar. Both the 1:0:6 and 1:0:6 + methyl cellulose mortars had an oversanded appearance and would have performed better with greater quantities of cementitious material. More work is required to investigate the influence of the water retention capacity of the mortar on the degree of hydration and the effects on microstructure and bond strength.

INTRODUCTION

One of the primary functions of the hardened mortar in unreinforced masonry is to provide structural integrity. This requires the mortar/unit combination to form a durable and adequate level of bond. The brick/mortar properties which influence the compatibility and bond forming process between the mortar and masonry unit are not yet fully understood. The bond forming mechanisms are complex and involve the flow of mortar fluids and fines to the brick/mortar interface followed by the hydration of the cementing materials. In order to identify some of these factors and to obtain a more thorough understanding of the bond forming process a collaborative research project into masonry bond has been in progress between CSIRO and the University of Newcastle. One strand of this research project has been dedicated to investigating the relationship between mortar microstructures and bond.

Studies investigating the bond between brick and mortar have been reviewed [Goodwin & West 1982]. Since then several investigations of the brick/mortar interface using optical and scanning electron microscopy have also been reported [Oppermann & Rudert 1983, Chase 1984, Lawrence & Cao 1987, Marusin 1990, Lange 1996, Sugo et. al. 1997]. Significant advances have also been made into the transport of fluids when fresh mortar contacts masonry units using techniques such as neutron absorption [Groot 1993].

Calcium silicate units are manufactured by an autoclaving process and rely on the hydrothermal reaction between calcium (quicklime) and silica (sand) to form the binding phase. Thus the mineralogy, surface topography and pore size distribution are quite different to those of fired clay products. When the units are laid, this could place different demands on the fresh mortar which may affect the bond strength development. In Australia, the difficulties in achieving an effective bond with calcium silicate units has resulted in the widespread recommendation to use methyl cellulose additive to enhance bond strength.

This study investigates the tensile bond strength/microstructure relationship for the combination of Portland cement based mortars and calcium silicate units. Optical and scanning electron microscopy are used to evaluate the nature of the microstructure together with X-ray diffraction and thermal analysis.

EXPERIMENTAL PROCEDURE

Only brief experimental details will be presented since these have been reported elsewhere [Sugo et. al. 1997]. Three types of mortar were used to investigate the effects of lime and methyl cellulose water thickener on the bond/microstructure relationship in combination with a commercially available calcium silicate unit. The reference mortar consisted of 1:0:6 (cement:lime:sand by volume). The two other mortars were a 1:1:6 and a 1:0:6 containing a methyl cellulose additive, recommended for mid-range IRA units. (The concentration used was 0.005 parts by weight of cement). The 1:1:6 mortar batch consisted of 11.2% (by weight) General Purpose Portland Cement, 4.8% hydrated lime and 84% sand; the 1:0:6

batches consisted of 11.7% Type GP cement and 88.3% sand. The sand used was a local washed and dried dune sand; its particle size distribution is shown in Table-1. Despite of the narrow size distribution and lack of fines this sand is used in masonry mortars due to its ready availability in the Newcastle area.

A period of 3-4 weeks was allowed for the units to equilibrate under laboratory conditions before construction of the brickwork couplets. The moisture content of the units at the time of laying was determined to be 2.9 ± 0.7 % (1std dev). The 24 hour cold water and 5 hour boil absorptions were determined to be 14.4 and 19.8% respectively. The IRA in the laboratory equilibrated condition was 1.33 ± 0.32 kg/m^2/min and in the oven dry condition 1.39 ± 0.30 kg/m^2/min. These properties were determined in accordance with AS/NZS4456 [Standards Australia, 1997]. The IRA values were measured for both bed surfaces for each of the ten units.

Twenty brickwork couplets were constructed for each mortar batch, with ten couplets from each batch being separated 1 hour after construction to evaluate the moisture distribution and the w/c ratio within the couplet. The fresh mortars properties of flow, cone penetration and gravimetric air content were determined in accordance with AS2701 [Standards Australia, 1984] and are presented in Table-2 together with the w/c ratio information and moisture distribution between the upper and lower units of the couplet and mortar joint.

The bond strength was determined from uniaxial tension specimens obtained by coring the brickwork couplets after curing for 7 days . Five 25mm diameter cores were removed along the center line of each couplet using a custom made thin walled diamond coring drill. The specimen details are given in Figure-1. For each brick/mortar combination, between 10 and 15 specimens were tested under a controlled rate of cross-head displacement of 0.5 mm/min. The maximum load and failure mode was recorded for each specimen.

After failure the fracture surfaces of the specimens were studied using an Olympus SZ6045 stereo microscope, with further investigations being carried out using a JEOL 840 Scanning Electron Microscope (SEM). Sawn, fractured and polished thin sections across the bed joints were also studied.

Mortar samples along the top and bottom interfaces were also taken for X-ray diffraction and simultaneous thermal analysis by removing a 2-3 mm mortar layer from the bed faces using a thin diamond lapidary saw. This process was carried out dry in order to avoid any possible dissolution of compounds. The mortar discs were then immediately crushed in a mortar and pestle to a fine powder. These powders were stored in small air tight containers in a desiccator to minimise any carbonation reactions. Powder X-ray diffraction patterns were obtained using a Philips PW1710 X-ray Diffractometer fitted with a Cu Kα tube. Scans were carried out in the 2θ range from 2 to 60 degrees using a step size of 0.020 degrees and 1 second duration. Simultaneous differential and thermogravimetric analysis were carried out using a SDT 2960 Simultaneous DTA/TGA from TA Instruments. A heating rate of 10°C/minute was used from room temperature to 1000°C in a static air atmosphere. The nominal sample mass was 15mg.

RESULTS

Fresh Mortar Properties and Moisture Distribution

The 1:0:6 + methyl cellulose and 1:1:6 mortars showed better workability than the 1:0:6 mortar. The 1:0:6 mortar was prone to segregation and was thus harder to work with. The addition of methyl cellulose overcame this tendency although the 1:1:6 mortar had an overall better workability. The 1:0:6 + methyl cellulose batch also showed slightly higher air content. Table-2 presents a summary of the fresh mortar properties, the initial w/c and 1 hour w/c ratios. The 1 hour w/c ratio represents an estimate of the moisture retained by the mortar which is available for the initial hydration of the cement constituents. The 1 hour w/c ratios vary considerably for the three mortars, with the w/c ratio for the 1:0:6 mortar being extremely low. The mean distribution of moisture within the couplets is also given in Table-2. It is apparent that both methyl cellulose and lime increased the moisture retention and also balanced the distribution of moisture between the bottom and top units.

Uniaxial Tests and Modes of Failure

The range of bond strengths and mode of failure are presented in Table-3. These values are 7 day tensile strengths and are arranged by the couplet source. Relatively high tensile bond strength values were achieved with the 1:1:6 mortar. The common mode of failure for this mortar was primarily along the mortar/unit interface although some mortar cohesive and masonry unit cohesive failures were also observed. The 1:0:6 mortar showed somewhat lower strengths with a primarily mortar cohesive mode of failure. Usually failure occurring a short distance away from the interface with some samples failing at the centre of the bed joint. The 1:0:6 + methyl cellulose mortar showed the lowest strengths, and these were all mortar cohesive failures. Some samples failed whilst being placed on the universal testing machine and thus it has not been possible to report these very low values.

Optical and Scanning Electron Microscope Studies

Examination of the sawn sections under the optical microscope showed clearly the significant contribution to the volume of paste by the lime component of the 1:1:6 mortar. In this mortar the sand grains were well coated with paste and good continuity of contact could be observed along the top and bottom brick interfaces. Occasional entrapped air voids 1-2 mm in diameter could also be observed.

Both of the 1:0:6 based mortars had an oversanded appearance with small volumes of paste providing cohesion between the sand aggregate. The presence of paste was limited to groups of sand particles which must have formed favourable capillary spacings in order to retain the paste against the brick suction effects. A dense and continuous dark grey band of cement paste could be observed along the top and bottom interfaces of the 1:0:6 + methyl cellulose mortar. A similar dark band could also be observed along the bottom interface for the 1:0:6 mortar whilst contact along the top brick interface only occurred in sections.

The 1:1:6 uniaxial tension test failures along the interfaces revealed a relatively smooth and uniform plane of paste in contact between the mortar and masonry bed face. The only features were small air voids (≈0.2 mm in dia.) and areas where the surface of the masonry unit had been pulled away with the mortar. The mortar cohesive fracture surfaces of the 1:0:6 and 1:0:6 + methyl cellulose mortars showed small quantities of paste bridging the sand aggregate together with no noticeable differences in the quantities of paste available. Comparing the interface adhesive failures of the 1:1:6 to the 1:0:6 mortar, the latter were rougher in appearance due to regions were the mortar had failed cohesively exposing the underlying sand aggregate particles.

Observations of the polished sections at low magnifications in the SEM confirmed the relative differences in the distribution of paste for the three mortars. It must be pointed out however that local variations in the distribution of paste and presence of voids do occur within each section. The polished section of the 1:1:6 mortar showed good contact along the bottom and top interfaces with the paste flowing into the surface texture of the unit. The sand particles within the mortar were closely spaced and showed good cohesion due to the well developed bridges of paste between the particles. Contact being made along more than one side of each particle as shown in Figure-2 which represents the mortar/bottom unit section. Comparing this figure to Figure-3, the 1:0:6 mortar section, the packing of the sand particles is reduced with an accompanying reduction in the connectivity of the particles. The layer of cement paste along the interface can also be seen. Figure-4 represents the 1:0:6 + methyl cellulose mortar/bottom masonry unit section, again showing the layer of cement paste along the interface. Contact between the sand grains has been further reduced with many particles only making point contact.

Also note the porosity and sandy nature of the calcium silicate unit itself, seen in Figures 2-4. The sand particles being the same grey level and of similar shape and size to that of the beach sand used in the mortar. The larger particles with various grey levels are finely crushed blue metal aggregate, the grey levels represent compositional variations within the multi-phase particles. A reaction rim can also be observed around each particle, representing the hydrothermal reaction products which form the binding phase of the unit.

The microconstituents of the fracture surfaces from the uniaxial specimens were investigated at high magnifications using the SEM. The interface adhesive failures of the 1:1:6 mortar allowed the microconstituents at the interface to be studied. Individual cement particles could be observed covered with a fluffy calcium silicate hydrate (CSH hydration products) and some rod shaped CSH. Some larger rod shaped structures possibly ettringite were also visible. Only small quantities of $Ca(OH)_2$ could be observed, generally as well shaped hexagonal crystals of about 8μm in diameter and 2-3μm thick. Observations of the 1:0:6 mortar samples which failed adhesively allowed a comparison of the CSH products formed at the interface. Here the cement grains were also covered with fluffy hydration products with only the occasional poorly developed rod shaped CSH structure.

The mortar cohesive failures of the 1:0:6 and 1:0:6 + methyl cellulose mortars were also investigated. At moderate magnifications the patchy cover of cement particles could be

observed on the surfaces of the sand aggregate. With higher magnification the nature of the hydration products could be observed. The hydration products for both mortars were very similar and consisted of Type I CSH fibrous particles (distinct from rod shaped CSH). The hydration products had developed sufficiently to provide intergrowth between the cement grains. Some platy hexagonal grains (≈10μm across and ≈0.1μm thick) were also visible in the 1:0:6 + methyl cellulose mortar. The nature of these crystals was not clearly identified since $Ca(OH)_2$ crystals do not usually have such high aspect ratios.

X-ray Diffraction and Thermal Analysis

The binding phase for the calcium silicate masonry unit was identified by XRD to be 11Å tobermorite. Other phases were also identified such as quartz (low), calcite ($CaCO_3$), calcium hydroxide and feldspar minerals the latter being associated with the blue metal aggregate. A sample of the beach sand used in the mortar batches was also identified to consist of quartz (low).

The XRD diffraction patterns for the three mortars also showed the peaks associated with the low form of quartz originating from the sand aggregate. Some of the major peaks from unreacted C_3S at 2θ values of 32.1, 32.6, 34.3, 34.4° were also present on the 1:0:6 and 1:0:6 + methyl cellulose patterns. The C_3S peaks at 34.3 and 34.4° were swamped on the 1:1:6 mortar trace by the presence of the main Portlandite ($Ca(OH)_2$) peak at 34.1°, which also has strong reflections at 18.1 and 47.1°. These $Ca(OH)_2$ peaks are essentially absent from the 1:0:6 and 1:0:6 + methyl cellulose patterns.

Another common peak in all three patterns was at the 2θ value of 29.3-29.4°. This peak may be a combination of the $CaCO_3$ peak (29.4°), one of the many CSH peaks in the 29° range or one of the secondary C_3S peaks at 29.6°. Two other peaks also remain unidentified, being at 42.4° on the 1:0:6 and at 27.5° on the 1:0:6 + methyl cellulose patterns respectively.

Thermogravimetric and differential thermal analysis (TGA/DTA) monitors the changes in mass and the endothermic or exothermic nature of any reaction which occurs as the sample is heated. This information is used to complement the XRD results. Given the mortar components; sand (silica), lime, Portland cement and its hydration products, numerous reactions would be expected.

The reactions observed in the three mortar samples are summarised in Table-4. The small quantities of methyl cellulose added as a water retainer would be beyond the limit of resolution in such an analysis. The main differences between the three mortars were at 450°C, 680°C and 890°C. The 1:1:6 mortar sample showed a 0.47% mass loss and endothermic reaction at 450°C due to the presence of $Ca(OH)_2$, with the 1:0:6 + methyl cellulose mortar showing only a trace of this endothrem due to the formation of $Ca(OH)_2$ primarily from the hydration of C_3S. Significants amounts of $CaCO_3$ were detected in all three mortars, with the mass losses at 680°C of 1.6, 0.54, 0.38% for the 1:1:6, 1:0:6 + methyl cellulose and 1:0:6 samples respectively. The higher portion of $CaCO_3$ in the 1:1:6 mortar is likely to be a result of the presence of $CaCO_3$ in the bagged hydrated lime. The

presence of $CaCO_3$ in the 1:0:6 based mortars would imply that the $Ca(OH)_2$ hydration by-product reacts readily with atmospheric CO_2 rather than remaining as a hydrate. The conversion of CSH to wollastonite (≈890°C) was exhibited by all three mortars, being more defined in the 1:1:6 mortar sample.

DISCUSSION

Masonry Unit Properties

The binding phase of calcium silicate masonry unit used in this study was identified by XRD to be 11Å tobermorite. The tobermorite reaction rim around the sand particles may be seen in the polished sections, Figures 2-4, within the masonry unit regions. At high magnifications the tobermorite structure may be observed to consist of a fibrous network, with the fibres being generally 5-10μm long and ≈1μm thick. The cross section of the fibres varied from rounded to rectangular in nature. Thus the surface of this type of unit is essentially a fine mesh which would allow a uniform flow of mortar fluids when in contact with fresh mortar and also allow a high degree of mechanical interlocking due to the mesh nature of the surface.

This type of structure would also have a different pore size distribution to that of fired clay units. The larger capillary pores may be seen in Figures 2-4, to consist of the interstitial spaces resulting from the packing of the sand particles. Smaller capillaries, in the order of a few microns, would also be present in the reaction rim around the sand particles due the arrangements of the tobermorite fibres. Finally, substantially smaller capillaries would exist in the order of Ångstroms (10^{-10} m) due to the nature of the tobermorite structure (which would be absent in fired clay products). These smaller capillaries would give calcium silicate units a greater suction potential which is not measured by standard suction tests such as the initial rate of absorption. The higher suction potential is likely to affect the mortar/brick water transport over an extended period of time.

Fresh Mortar Properties

A comparison of the fresh mortar properties may be made from Table-2. The 1:0:6 + methyl cellulose mortar required a slightly lower initial w/c ratio to produce a workable mix. The addition of methyl cellulose also reduced the tendency of the mix to segregate shown by the 1:0:6 batch. The bulk density of the fresh mortar was also reduced with the methyl cellulose addition. The addition of lime increased slightly the bulk density relative to the 1:0:6 batch and also improved the workability of the mortar. The 1 hour w/c ratios show the relative influence of the methyl cellulose and lime additives on the moisture retentivity of the mortar over an extended period of time. The very low (0.08) 1 hour w/c ratio for the 1:0:6 batch is significantly improved by the addition of methyl cellulose to a value of 0.22. Lime has an even stronger effect and increased the 1 hour w/c ratio to 0.35.

The addition of methyl cellulose and lime to the mortar batches also affected the distribution of moisture within the couplets, as shown in Table-2. The role of these additives was to

balance the moisture distribution between the top and bottom masonry units. These differences confirmed the flow of paste to the interfaces observed in the sawn and polished sections. Both the 1:0:6 + methyl cellulose and 1:1:6 mortars had an even distribution of paste along the bottom and top brick/mortar interfaces. The 1:0:6 batch showed a greater quantity of paste along the bottom interface corresponding to the higher quantity of moisture attracted to by the bottom unit. Whilst further work needs to be carried out to clarify this mechanism, it would appear that the mortar fluids either settle out by segregating or the effect results from the mortar being placed on the bottom unit first before the upper unit is layed, thus producing different contact times at the two interfaces.

Bond Strength and Mode of Failure

The results from the uniaxial tension tests shown in Table-3 indicate that the 1:0:6 mortar was still able to produce reasonable levels of bond (0.87MPa) given the extremely low 1 hour w/c ratio and the uneven top/bottom paste distribution. This uneven paste distribution may explain why some of the specimens failed along the top unit interface, however the common failure mode was mortar cohesive either at the centre of the joint or 2-3mm away from the unit interface. Both the 1:0:6 and the 1:0:6 + methyl cellulose mortar, which had a much higher 1 hour w/c ratio, showed similar microstructures at high magnifications. This was also verified by the similarities in the XRD patterns and DTA/TGA plots, although the methyl cellulose mortar showed a slight trace of the $Ca(OH)_2$ endotherm at 450°C. Thus it would appear that despite the initial differences of the low w/c ratio, sufficient moisture has been available in both cases to allow the mortars to develop similar levels of hydration. The source of this moisture is likely the flow reversal phenomenon which has been previously reported [Groot, 1993].

The observed bond strength and mode of failure for the 1:0:6 + methyl cellulose mortar are more difficult to interpret. Given the better distribution of moisture/paste along the top and bottom interfaces, a higher w/c ratio, and a similar microstructure to the 1:0:6 mortar, similar if not better bond strengths should have resulted. However the measured strengths were generally only 30-40% of those shown by the 1:0:6 batch. The mode of failure indicated that these were mortar cohesive strengths with failure occurring 2-3mm away from the interface. This lower mortar cohesive strength may be explained by the initial lower bulk density and the reduced cohesion of the sand aggregate shown in Figure-4. This is only a qualitative observation and detailed image analysis would be required to establish this. Examination of the polished sections for the 1:0:6 and 1:0:6 + methyl cellulose mortars reveals that both of these mortars would be expected to perform better if greater quantities of cementitious paste were available, as would be the case in 1:0:5 or 1:0:4 mixes. (It is significant to note that these are also the proportions recommended by the water retainer manufacturer).

The 1:1:6 mortar had a greater volume of paste which increased the cohesive strength of the mortar, and consequently most failures occurred adhesively at the brick/mortar interface. The mean bond strength was 1.29MPa and exceeded the cohesive tensile strength of the calcium silicate unit in some of the samples. Examination of the polished section, (Figure-2) shows good contact being made along the interface and well developed cohesion due to the

larger area of contact between the sand aggregate particles. The hydration products observed at the interface appeared to be more reacted than those observed in the interface failures of the 1:0:6 mortar. Some differences are apparent when the microconstituents found at the interface of the 1:1:6 mortar/calcium silicate unit combination are compared to those previously reported for the same mortar in combination with an extruded clay unit of similar IRA [Sugo et al 1997]. The main difference appears to be in the quantity of $Ca(OH)_2$ and in the density and size of the CSH rod shaped structure. With the extruded clay unit large areas of $Ca(OH)_2$ could be observed at the interface, whilst only small grains could be observed for the mortar in contact with the calcium silicate unit. Similarly, the rod shaped CSH structure with the clay unit was well developed and very dense with the rods generally aligned perpendicular to the interface. The rod shaped CSH structure in the calcium silicate combination was not as dense and there was no apparent preferred orientation. Despite the magnitude of these differences, the observed bond strength for the 1:1:6 mortar in combination with the extruded clay unit was only marginally higher, 1.37MPa compared to 1.29MPa for the calcium silicate unit.

Degree of Hydration

Estimating the degree of hydration by such means as scanning electron microscopy is difficult and also subjective. The use of techniques such as XRD and DTA/TGA complement the optical and SEM investigations. However the large quantities of silica in the mortar samples (84-88% by weight) reduces the sensitivity of such analysis. XRD has shown that for all three mortars some C_3S has remained unreacted, indicationg that some potential for improvement in strength exists if hydration was able to continue. DTA/TGA analysis indicated that more hydration has occurred in the 1:1:6 mortar sample which supports the SEM observations. This may be due to the influence of lime in retaining a higher relative humidity within the mortar as the rate of hydration decreases once the RH drops below 100%, with no hydration occurring below 85%RH.

CONCLUSIONS

This study investigated the bond strength/microstructure relationship for three Portland cement based mortars in combination with a calcium silicate masonry unit. The methyl cellulose and lime additives improved the workability and water retentivity of the mortars. Different bond strengths were observed for the three mortars with the highest strength shown by the 1:1:6 mortar. The observed bond strengths were not just related to differences in the hydration products but also and perhaps more importantly to the quantity and distribution of paste. It is likely that the lower bond strengths shown by the 1:0:6 and especially the 1:0:6 + methyl cellulose mortar could be improved with greater quantities of cementitious material. The presence of unreacted C_3S in all three mortars at 7 days may lead to strength gains if sufficient moisture is available for hydration to continue. Thus additional research is required to investigate the effect of the mortar moisture content on the rate of hydration and the influence on bond strength/microstructure. Results from this investigation tend to indicate that bond strength (or mortar cohesive strength) is significantly influenced by the macroscale events like the quantity and distribution of cementitious material.

ACKNOWLEDGEMENTS

This work was partly funded by the Australian Research Council whose support is gratefully acknowledged.

REFERENCES

Chase, G.W., 1984. Investigations of the Interface Between Brick and Mortar, The Masonry Society Journal, Vol. 3, No. 2, pp. T1-T9.

Goodwin, J.F. & West, W.H., 1982. A Review of the Literature on Brick/Mortar Bond. Proc. of the British Ceramic Society, Vol. 30, No. 23, pp. 23-37.

Groot, C.J.W.P, 1993, Effects of Water on Mortar-Brick Bond. Delft University of Technology, Delft, The Netherlands.

Lange, D.A., DeFord, H.D. & Ahmed, A., 1996. Microstructure and Mechanisms of Bond in Masonry. Proc. 7th North American Masonry Conference, University of Notre Dame, South Bend, Indiana, June, pp. 167-174.

Lawrence, S.J. & Cao, H.T., 1987. An Experimental Study of the Interface Between Brick and Mortar. Proc. of the 4th North American Masonry Conference, Los Angeles.

Marusin, S.L., 1990. Investigations of Shale Brick Interface with Cement-Lime and Polymer Modified Mortars. ACS, Vol. 73, No. 8, pp. 2301-2308.

Oppermann, B., Rudert, I., 1983. Untersuchungen zur Verbesserung des Haftverbundes Mörtel/Stein. Zement-Kalk-Gips, Vol. 36, No. 1, pp. 43-50.

Standards Association of Australia, "Methods of Sampling and Testing Mortar for Masonry Construction- AS2701-84". "Masonry Units and Segmental Pavers-Methods of Test, AS/NZS 4456-97", Homebush, NSW, Australia.

Sugo, H.O., Page, A.W. & Lawrence, S. J., 1997. Characterization and Bond Strengths of Mortars with Clay Masonry Units. Proc. 11th IB^{2}MC, Tongji University, Shanghai, China, pp. 59-68.

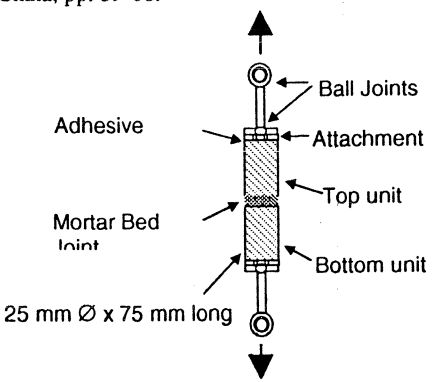

Figure-1. Brickwork Specimens Tested in Uniaxial Tension.

Table-1. Particle Size Distribution of Dune Sand.

Sieve Size	% Passing
2.36mm	100
1.18mm	100
600μm	96
300μm	25
150μm	1
75μm	0

Table-2. Fresh Mortar Properties, 1 Hour W/C Ratios and Moisture Distributions.

Mortar Type	Flow (%)	Cone Penetration	Gravimetric Air Content (%)	Bulk Density (kg/m^3)	Initial w/c Ratio	1 hour w/c Ratio*	% Moisture Distribution at 1 Hr (top /mortar/bottom)
1:0:6	110	60	4	1980	1.84	0.08±0.01	39/4/57
1:0:6 + methyl cellulose	90	50	10	1920	1.58	0.22±0.04	42/13/45
1:1:6	110	60	3	2020	1.82	0.35±0.08	40/20/40

* ± 1 standard deviation

Table-3. Direct Tension Test Results of Calcium Silicate Specimens.

Couplet	1:0:6 Mortar		1:1:6 Mortar		1:0:6 + methyl cellulose Mortar	
No.	Bond Strength (MPa)	Failure Mode	Bond Strength (MPa)	Failure Mode	Bond Strength (MPa)	Failure Mode
1	0.89	M/C 2-3mm ↓ TI	1.44	I/A TI	0.40	M/C 2-3mm ↓ TI
	0.98	M/C CJ	1.17	I/A TI	0.07	M/C 1-2mm ↑ BI
2	0.87	M/C 2-3mm ↑ BI	1.19	M/C CJ	0.22	M/C 1-2mm ↑ BI
	0.73	I/A T/I	1.29	M/C CJ	0.24	M/C 1-2mm ↑ BI
	0.81	I/A T/I	0.89	M/C CJ	0.10	M/C 1-2mm ↑ BI
	0.94	M/C 2-3mm ↓ T/I				
3	1.20	M/C CJ	1.23	I/A BI	-	Failed prior to testing
	1.22	M/C CJ	1.42	I/A BI	0.13	M/C 2-3mm ↓ TI
			1.46	I/A BI	0.15	M/C 2-3mm ↓ TI
4	0.79	M/C 2-3mm ↑ BI	1.37	I/A BI	0.17	M/C 2-3mm ↑ BI
	0..71	M/C 1-2mm ↑ BI	1.16	U/C 2mm ↑ TI	-	Failed prior to testing
	0.84	M/C CJ			0.21	M/C 2-3mm ↑ BI
	0.80	M/C 2-3mm ↓ TI				
	0.52	M/C 2-3mm ↑ BI				
5	0.91	M/C CJ	1.49	U/C 2mm ↑ TI	0.59	M/C 2-3mm ↓ TI
	0.87	M/C 2-3mm ↓ T/I	1.34	U/C 2mm ↑ TI	-	Failed prior to testing
			1.38	U/C 2mm ↑ TI	0.68	M/C 2-3mm ↓ TI
					0.77	M/C CJ
Mean	0.87, std dev. 0.18		1.29, std dev. 0.16		0.31, std dev. 0.24	

M/C= Mortar Cohesive Failure U/C= Unit Cohesive Failure I/A= Interface Adhesive Failure
↑/↓ = Up/Down BI= Bottom Interface TI= Top Interface CJ= Centre of Joint

Table-4 Summary of Reactions Observed by DTA/TGA on Mortar Samples.

Temperature	Event
<100°C	Moderate endotherms + mass loss- removal of adsorbed moisture
130-230°C	A series of small endotherms + gradual mass loss- partial dehydration of CSH
≈450°C	Strong endotherm and mass loss- dehydroxylation of $Ca(OH)_2$
574°C	Sharp endotherm- $\alpha \rightarrow \beta$ quartz transformation (sand)
≈680°C	Strong endotherm + mass loss-decomposition of $CaCO_3$
≈890°C	Weak exotherm- re-arrangement of dehydrated CSH→wollastonite ($CaSiO_3$) phase

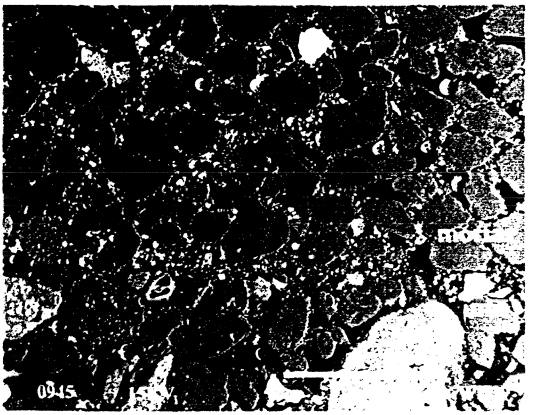

Figure-2. 1:1:6 Mortar/Unit Polished Section.

Showing the cross section of the bottom bed joint, note the good distribution of paste along the interface and the large areas of contact between the sand particles filled with paste. Secondary electron image, bar length = 1mm.

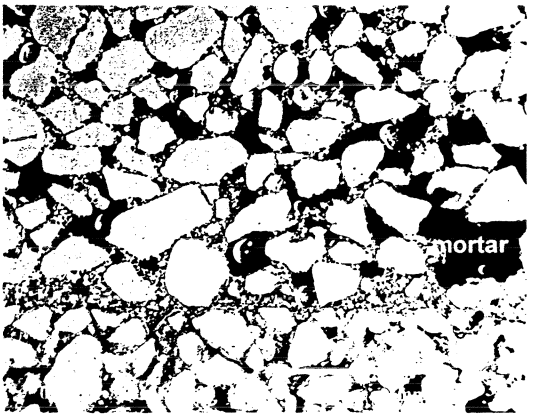

Figure-3. 1:0:6 Mortar/Unit Polished Section.

The flow of paste to the interface may be observed. Note the reaction rim around the sand particles and void areas between the sand particles within the masonry unit. The shape and size distribution of these particles is similar to those of the beach sand used in the mortar batch.
Secondary electron image, bar length = 1mm.

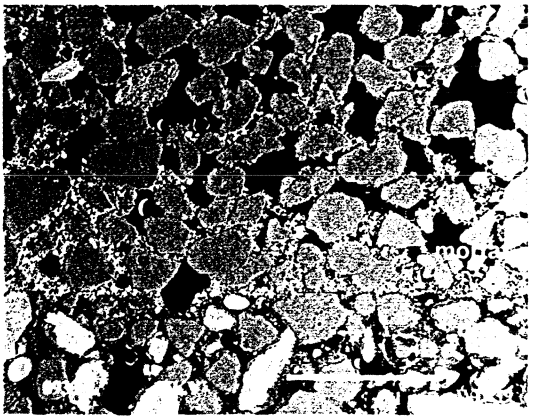

Figure-4. 1:0:6 + Methyl Cellulose Mortar/Unit Polished Section.

Note the flow of paste to the interface and the reduced cohesion between sand particles, with some particles only making point contact.
Secondary electron image, bar length = 1mm .